Journal of Engineering Science and Technology
Special Issue on Development of Sustainability Systems - I, 18 - 32

PERFORMANCE ASSESSMENT OF EJECTOR REFRIGERATION SYSTEM UNDER VARIOUS OPERATING CONDITIONS

AMGED AL EZZI[1], HANEEN H. RAHMAN[2], HASANAIN A. ABDUL WAHHAB[3,*]

[1]Department of Electromechanical Engineering, University of Technology- Iraq, Baghdad, Iraq
[2]Department of Mechanical Engineering, Wasit University, Wasit, Iraq
[3]Training and Workshop Centre, University of Technology- Iraq, Baghdad, Iraq
*Corresponding Author: 20085@uotechnology.edu.iq

Abstract

A supersonic ejector system is proposed as an alternative to the mechanical compression system in wide industrial cooling/refrigeration applications due to lower power system consumption. Detailed information is lacking to mimic the system design performance under different operation conditions, particularly with the mathematical modeling investigation. This study develops a new mathematical model to simulate the coefficient of cooling performance under several Mach numbers, condensation temperature, and coolant mass flow rate. The study outcomes show that the ejector operating temperature is a key design parameter affecting cooling performance. In addition, the mathematical model shows that the optimum nozzle exit Mach number started with is 2.6 for each selected mass flow rate ratio. Results show that starting with a higher nozzle exit pressure than the secondary flow stagnation pressure value than condenser pressure was normal pressure value and starting with a higher will make the saturated condenser pressure very high and, as a result, decline in the cooling performance.

Keywords: Cooling effect capacity, Cooling system performance, Ejector nozzle, Mathematical modeling, Refrigeration cycle.

1. Introduction

A steam ejector-cooling device is a very effective cooling method, which has been progressive since 1901 when Le Blanc and Parson built the first steam jet refrigerator system [1]. Power energy problems patrol and the gas problem led to start to think about connecting renewable energy sources with effective thermal management solutions. An ejector cooling system combines the most important two points all engineers seek for acceptable working efficiency and low cost. The system comprises a boiler, nozzle, diffuser, condenser, and evaporator. The ejector work is affected by different parameters, such as the dimensions of the system components and the operating temperature, which limits the coefficient of operating performance. There are many efforts and tries to develop the ejector performance. Chunnanond and Aphornratana [2] summarized the ejectors and their applications in refrigeration. They concluded that the understanding of the ejector theory had not been completely cleared to enhance the efficiencies and reduce the cost of the ejector cooling system. The review by Sun and Eames outlined the developments in mathematical modeling and design of the jet ejector. Zhang and Wang [3] and He et al. [4] presented a mathematical model that can be classified into two categories (a) steady thermodynamic subdivided into single-phase flow and two-phase flow (b) dynamic, which has higher prediction. Two theorems have been used in the ejector design [4, 5].

The first is the constant area, and the second is the constant pressure. The obstacle the designers have been working on is getting good COP value with a wide condenser saturated temperature range. The designers have built different models to see the effect of fixing parameters and changing the other. Many computer mathematical models have been modeled because it is very important to reduce the time of the experimental trying. In line with this, Scott et al. [6] describe an experimental test bench using R245fa assembled and operated at Canmet ENERGY in Varennes. Mansour et al. [7] conjugate effects of the thermal and mechanical compression component's interactions on the system performance were investigated. The study was validated between the ejector model and the manufacturer's compressor, which e numerical results have provided good and useful information on cycles working under a refrigeration configuration and integrating ejectors.

Evaluation of the effectiveness of the system of the ejector charge air-cooling is possible theoretically and empirically was introduced by Lazarev et al. [8]. The result appeared that the effectiveness of the system ejection charges air cooling of 'air-to-air' type on each engine operation parameters, ratio ejection coefficient efficiency, and thermal cooling efficiency are very important parameters that affected ejector performance. Purjam et al. [9] from Kyushu University- Japan, proposed an extra turbo expander, compressor, and gas cooler integrated with the conventional ejector model. The study found that pressurizing the secondary entrance of the ejector could be beneficial to cooling performance, and using the expansion process right after the ejector can potentially increase the COP system. The literature shows that many researchers have introduced experimental, mathematical, and CFD studies describing the cooling ejector compounds and development. However, more detailed information is needed to simulate the system design performance under different operation conditions.

This study aims to evaluate a new mathematical model to simulate the behavior of the coefficient of cooling performance under several Mach numbers, condensation temperature, and coolant mass flow rate.

2. Methodology and Modelling

The ejector cooling system essentially connects the work of the main components, which include a boiler, nozzle, mixing chamber, diffuser, condenser, and evaporator. The idea is to create a pressure difference between the steam exit from the nozzle and the condenser, which will make the water vapor in the steam able to condense and go back to the boiler to start the cycle again. The condensation water, which comes from the condenser, will return to the low-temperature evaporator, which creates the second steam flow, and the rest will go to the high-temperature boiler and create the primary steam flow. The evaporator and the boiler parts represent the criteria of the ejector performance, which is the amount of energy added to the boiler compared to the energy removed from the evaporator. To create the pressure difference, the importance of using nozzle converge-diverge shows up because the exit flow of the steam needs to be supersonic (Ma > 1) considering the second flow's pressure. The exit flow from the nozzle needs to be supersonic to make it low pressure, and that will lead to creating a vacuum force that helps to draw the secondary flow to the nozzle exit area and then to the mixing chamber, as shown in Fig. 1.

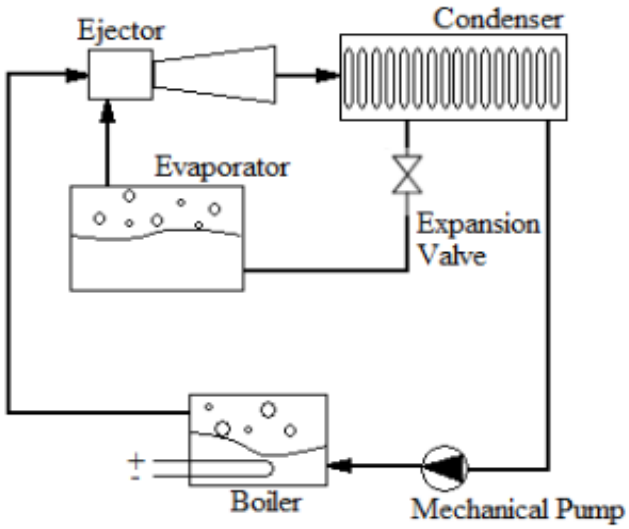

Fig. 1. Schematic diagram of ejector cooling system.

The pressure of the secondary flow at the nozzle's exit will be the same as the nozzle exit, depending on the theory of constant pressure design, which helps in designing the area [5]. Then, the primary and secondary flow will enter the mixing chamber area where the flow properties such as the mass flow rate, velocity, and Mach number will change to become mixing properties. By the end of the mixing chamber, the two streams are completely mixed, and the static pressure is assumed to remain constant until it reaches the constant area tube section. The mixing flow will go through a constant area tube, and then it will face a normal shock wave due

to the high pressure in the back of the system, specifically at the condenser side. The flow properties after the normal shock will change, especially the pressure and flow speed. After the normal shock, the pressure increases. The velocity decreases from supersonic to subsonic, and here, the necessity of using a diffuser increases the back pressure, which is the same as condenser pressure. Still, this increase must be reasonable and does not exceed the design limitation because that will make the normal shock move and could reach the nozzle position and stop the system running [6].

It can be observed that the steam flow has three main components passing through them. The nozzle, mixing chamber, and diffuser are undergoing isentropic flow relations due to no heat being added or removed from the flow in those three components. Having two flow streams with sonic and supersonic speed, normal shock, and pressure difference during the system makes the ejector design very complex. It needs a reasonable assumption and a sophisticated mathematical model to reduce the design time, as shown in Figs. 2 and 3.

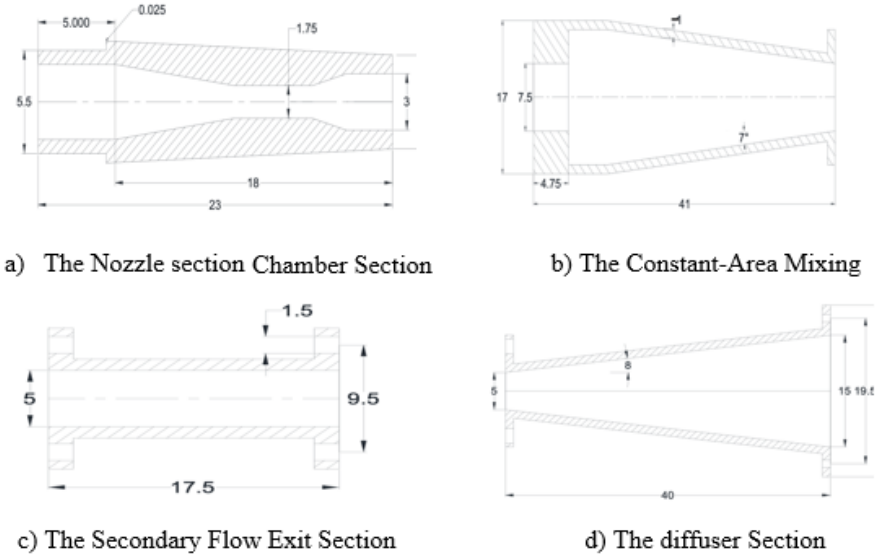

Fig. 2. Ejector cooling isentropic sections.

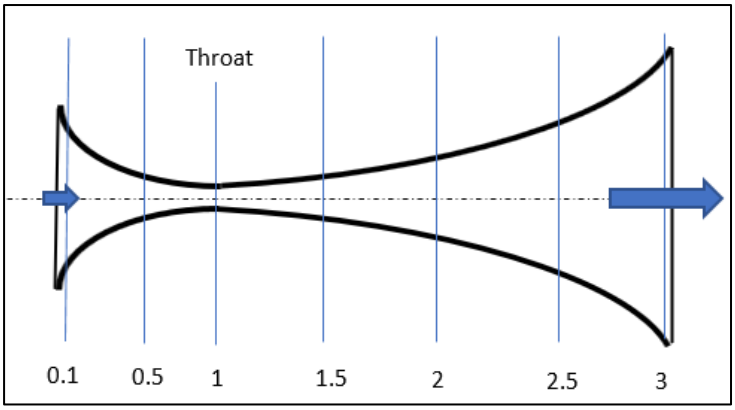

Fig. 3. Gradient of the Mach number through the nozzle.

The constant pressure design is based on the following assumptions. The primary and secondary flows are the same fluid: steam flow. The primary and secondary streams expand isentropic ally through the nozzles. In addition, the mixture stream compresses the isentropic ally in the diffuser. The primary and secondary fluid streams are saturated vapor, and their inlet velocities are negligible. The velocity of the compressed mixture leaving the diffuser is negligible. Constant isentropic expansion exponent and ideal gas behavior. The mixing of the primary and secondary vapor takes place in the mixing chamber and is completed before the presence of the shock wave. The walls of the ejector are considered an adiabatic boundary. The nozzle isentropic efficiency is (1), and the friction losses were defined in terms of isentropic efficiencies in the diffuser (0.98) and mixing chamber (0.97). At the nozzle exit, the pressure of the nozzle exit and the secondary flow are assumed to be uniform. The general flow governing equations must be used to build a mathematical model for ejector cooling [10-12].

Conservation of mass as the following equation

$$\sum \rho_i V_i A_i = \sum \rho_e V_e A_e \tag{1}$$

Conservation of momentum as the following equation

$$P_i A_i + \sum m_i V_i = P_e A_e + \sum m_e V_e \tag{2}$$

Conservation of energy as the following equation

$$\sum m_i (h_i + {}^{V_i^2}/_2) = \sum m_e (h_e + {}^{V_e^2}/_2) \tag{3}$$

From Eqs. (1) to (3), all the coming equations are driven based on isentropic assumption. The ejector coefficient of the performance (COP) is

$$COP = \frac{cooling\ load(evaporatoer)}{heating\ load(boiler)} \tag{4}$$

$$COP = \frac{\dot{m}_{sec.} h_{lv,s}}{\dot{m}_{prim.} h_{lv,p}} \tag{5}$$

The entrainment ratio, ω or the ratio of the entrained vapor mass flow rate to the mass flow rate of the primary fluid is:

$$\omega = \frac{\dot{m}_{sec.}}{\dot{m}_{prim.}} \tag{6}$$

When the ejector boiler and evaporator stagnation temperature is below 1000 ºC, the difference between $h_{lv,s}$ and $h_{lv,p}$ will be very small so that it could be neglected. Then, the entrainment ratio will be the same as the coefficient of performance.

ω = COP (7)

The following gas dynamic equations are frequently used in the ejector cooler design since the working fluid flow is compressible.

$\dot{\eta}_{nozzle} = 1$ (8)

$a = \sqrt{k * R * T}$ (9)

$Ma = \frac{V}{a}$ (10)

$\frac{T_o}{T} = (1 + \frac{k-1}{2} Ma^2)$ (11)

$\frac{\rho_o}{\rho} = \left(1 + \frac{k-1}{2} Ma^2\right) \times \frac{1}{\mathrm{K}-1}$ (12)

$\frac{P_o}{P} = \left(1 + \frac{k-1}{2} Ma^2\right) \times \frac{\mathrm{k}}{\mathrm{k}-1}$ (13)

$\dot{m} = \rho * V * A$ (14)

$A_n = \frac{\dot{m_p}}{\rho Ma\sqrt{kRT}}$ (15)

The primary steam flow properties through the nozzle could be obtained from [13, 14]. The flow temperature, pressure, density, and mass flow rate can be found for each nozzle point depending on the stagnation flow properties before the nozzle using the mathematical relations 6 to 15. Knowing the mass flow rate will help find the area of the nozzle sections for each Mach number. The second flow from the evaporator has stagnation properties such as pressure, temperature, and density. The idea of the nozzle design is that the nozzle pressure exit must be lower than the stagnation second flow pressure, but at the nozzle exit section, the pressure because of the theory of constant pressure design assumed to be unified and equal to the primary nozzle flow exit ($P_{1,p} = P_{1,s}$) [15, 16]. Thus, the second flow Mach number at the nozzle exit section before the mixing chamber is:

$M_{1,s} = \sqrt{\left(\frac{2}{k-1}\right)\left[\left(\frac{P_{o,s}}{P_{1,p}}\right)^{\frac{k-1}{k}} - 1\right]}$ (16)

The second flow area at any plane in the nozzle could be predicted from the area ratio, Eq. (17)

$\frac{A_{1,s}}{A_{1,p}} = \left(\frac{T_{o,s}}{T_{o,p}}\right)^{1/2} * \left(\frac{R_s}{R_p}\right)^{1/2} * \frac{f_{1,p}}{f_{1,s}} * \omega$ (17)

The gas constant and the heat-specific ratio of the flow in all the primary and secondary sections of the system are the same since it is assumed to be ideal. Hence,

Rs = Rp = Rm
and
ks = kp = km

$f_{1s} = M_{1,s}[k\left(1 + \frac{k-1}{2} M_{1,s}^2\right)]^{1/2}$ (18)

$f_{1,p} = M_{1,p}[k\left(1 + \frac{k-1}{2} M_{1,p}^2\right)]^{1/2}$ (19)

The flow properties in the mixing chamber, such as the mixture Mach number and the total mass flow, are very important to find the rest of the flow properties. To determine the Mach number of the mixture, Ma3, use conservation of momentum on a control volume enclosing the mixing chamber was used as [17] recommendation:

$$\dot{\eta}_m = 0.98$$

$$\dot{m_P} * V_{1,P} + \dot{m_s} * V_{1,s} = \dot{\eta}_m * \dot{m_m} * V_3 \tag{20}$$

Where number 3 is mentioned in the mixing chamber area just before the normal shock.

$$V_3 = \frac{1}{\dot{\eta}_m}\left[\frac{V_{1,P}+\omega * V_{1,s}}{1+\omega}\right] \tag{21}$$

After substituting Eq. (4) in Eq. (15), the chock mixture Mach number is:

$$M_3^* = \frac{1}{\dot{\eta}_m}\left[\frac{M_{1,p}^* + \omega * M_{1,s}^* \sqrt{\frac{k_s R_s T_{o,s}}{k_p R_p T_{o,p}}\left(\frac{k_p+1}{k_s+1}\right)}}{\sqrt{1+\omega}\sqrt{\frac{k_p+1}{k_p R_p (k_m+1)}}\sqrt{\frac{k_p R_p (k_m-1)}{(k_p-1)} + \omega \frac{k_s R_s (k_m-1)}{(k_s-1)}\left(\frac{T_{o,s}}{T_{o,p}}\right)}}\right] \tag{22}$$

where:

$$M_{1,p}^* = \sqrt{\frac{M_{1,p}^2 (k_p+1)}{M_{1,p}^2 (k_p-1)+2}} \tag{23}$$

$$M_{1,s}^* = \sqrt{\frac{M_{1,s}^2 (k_s+1)}{M_{1,s}^2 (k_s-1)+2}} \tag{24}$$

Then the mixture Mach number, Ma3, is:

$$Ma_3 = \sqrt{\frac{2*(M_3^*)^2}{[k+1-M_3^{*2}k+M_3^{*2}]}} \tag{25}$$

The mixing chamber area is:

$$\frac{A_m}{A_t} = (1+\omega)\frac{P_{o,p}}{P_3\sqrt{T_{o,p}}}\sqrt{R_m T_3}\frac{\sqrt{\frac{k_p \dot{\eta}_n}{Rp}\left(\frac{2}{k_p+1}\right)^{\frac{k_p+1}{k_p-1}}}}{f_3(k_m, M_3)} \tag{26}$$

Where the mixing temperature, T3, and the f3 are predictable from

$$T_3 = \frac{\frac{k_p R_p}{k_p-1} T_{o,p} + \omega \frac{k_s R_s}{k_s-1} T_{o,s}}{(1+\omega)\frac{k_m R_m}{k_m-1}} \tag{27}$$

$$f_3 = M_3\left[k\left(1+\frac{k-1}{2}M_3^2\right)\right]^{1/2} \tag{28}$$

The mixture flow Mach number and pressure before the normal shock are Ma3 and P3 with the same as the nozzle exit pressure P1, p, according to the theory of constant pressure design.

The flow after the shock wave will decelerate from supersonic (Ma >1) flow to subsonic flow (Ma <1), and the pressure will increase due to that decelerating. The Mach number after shock wave Ma4 is:

$$(\mathrm{Ma}_4)^2 = \left[\frac{(\mathrm{Ma}_3)^2 + \frac{2}{\mathrm{k}-1}}{\left(\frac{2\mathrm{k}}{\mathrm{k}-1}\right)(\mathrm{Ma}_3)^2 - 1}\right] \tag{29}$$

The pressure after the shock wave P4 is:

$$P_4 = P_3 \left[\frac{1+k(Ma_3)^2}{1+k(Ma_4)^2}\right] \quad (30)$$

where: $P_3 = P_{1,p}$

The mixture pressure is the same as the primary nozzle exit pressure. Then, these flow properties enter the diffuser section. The flow velocity through the diffuser will decrease more, and the flow pressure exit from the diffuser is very high, which is considered the same as the condenser pressure or backpressure Pb. The diffuser efficiency ήd assumed to be 0.97 [18].

The diffuser exit pressure (back pressure) is:

$$P_b = P_4[\frac{\dot{\eta}_d(k-1)}{2}\ (Ma_4)^2\ + 1]^{\frac{k}{k-1}} \quad (31)$$

The saturated condenser pressure is the same as the back pressure used to find the condenser's saturated temperature. The experimental ejector cooling circumstances are the amount of energy that is added to the boiler is 200 W. The evaporator stagnation temperature and pressure (secondary flow) are 10 ^{o}C and 1228 Pa, respectively. The condenser saturated temperature ranges between 25 and 40 ^{o}C. The stagnation boiler steam flow temperature, pressure, density, and velocity before the nozzle entrance are (To, Po, ρo, and Vo), respectively, as shown in Table 1. The inlet velocity is very small, so it will be neglected.

Table 1. Boundary conditions before the nozzle entrance.

To,p (^{o}C)	Po,p (pa)	ρo,p (kg/m3)	hlv,p (kJ/kg)	To,s (^{o}C)	Po,s (pa)	hlv,s (kJ/kg)
62	21670	0.141	2354	10	1228	2479

$\dot{m_p} = \frac{Q_{boiler}}{h_{lv}} = 8.5 \times 10^{-5}$ kg/s

Due to the stagnation boiler and evaporator temperature blowing 100 ^{o}C, the difference between the primary and secondary flow latent heat is very small. Thus, the coefficient of the performance of the ejector will be:

$$C.O.P = \frac{\dot{m_{sec.}} h_{lv,s}}{\dot{m_{prim.}} h_{lv,p}} \quad \text{or} \quad C.O.P = \omega * \frac{h_{lv,s}}{h_{lv,p}}$$

Thus, the COP will be the same as the entrainment ratio, ω.

$$\omega = \frac{\dot{m_{s.}}}{\dot{m_{p.}}}$$

Choosing the entrainment ratio or mass flow ratio is the key to designing the ejector system's whole sections. Because to find the section area, it is important to know the mass flow rate in the section. The mathematical model helps to show picking different entrainment values affects the condenser pressure, which is related to the condenser temperature. Because the flow exit from the nozzle needs to be supersonic, a converge-diverge nozzle has been used [19-23]. The flow velocity through the nozzle converges section will gradually increase until it reaches the maximum at the throat chock point, where the Ma = 1. Then, the flow velocity through the nozzle diverge section will continue increasing until the supersonic flow at the exit. The area of the nozzle is a function of the Mach number and the mass flow rate. Thus, the area found by applying different Mach numbers in the nozzle equations with. Due to the velocity before the nozzle entrance is considered to be almost zero [24, 25], the Mach number at the nozzle entrance was

picked as 0.1 subsonic and then gradually increased to make it sonic at the throat chock point, and continuing to make it supersonic at the exit. The restrictions of picking the nozzle exit Mach number are: the primary steam flow exit from the nozzle needs to be lower than the second flow stagnation pressure; the condenser saturated temperature, which is affected by the condenser-saturated pressure, needs to be in the range of 25 to 40 ºC.

3. Results and Discussion

The mathematical model shows that the nozzle exit Mach number must be started with 2.6 for each selected mass flow rate ratio, ω, because starting with a Mach number below this value will give the nozzle exit pressure value higher than the secondary flow stagnation pressure value. In addition, it shows that going further in Mach number will make the saturated condenser pressure very high, and that will cause two things. First, the normal shock will move toward the nozzle, stopping the system been working. Second, the condenser-saturated temperature will be very high, out of the limiting range, as shown in Figs. 4 and 5.

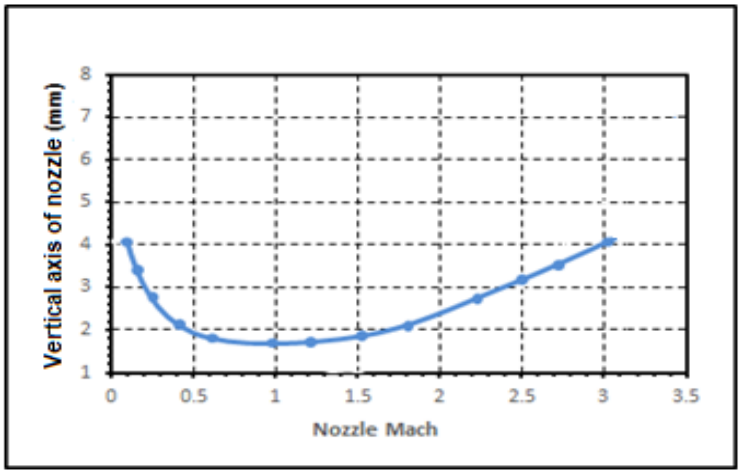

Fig. 4. Nozzle vertical axis changing with Mach number in each section.

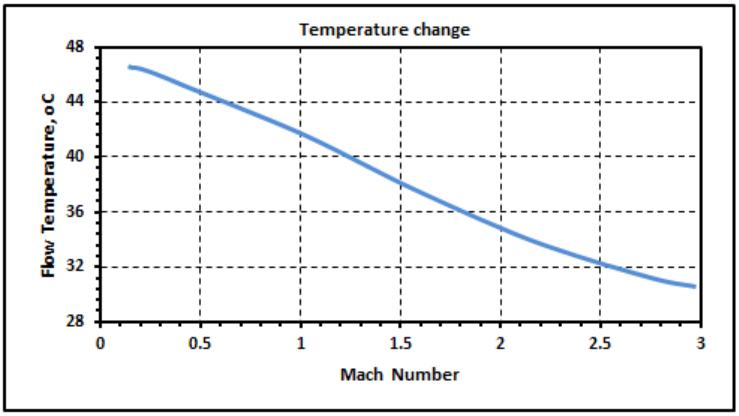

Fig. 5. Temperature drop through the nozzle.

Figure 6 shows the relationship of pressure drop between the inlet and outlet of the nozzle at different Mach numbers. The parabolic shapes represent these relations. The optimum working point done at M = 1.5 and the ratio of pressure = 0.6 is of lower power generation. The left side for this number is (in the figure) the area of the higher pressure drop irreversibility effect. In contrast, the right side is the irreversibility effect of lower pressure drop. The figure shows the Bejan result matches the highest range of critical Mach number, where the friction irreversibility effect part and between the fourth and third range in the energy irreversibility effect part for this study. Theoretical results showed that the difference in inlet and outlet pressure decreases with increasing Mach number, with the decreasing percentages being 9.6%, when changing the Mach number to 3.0.

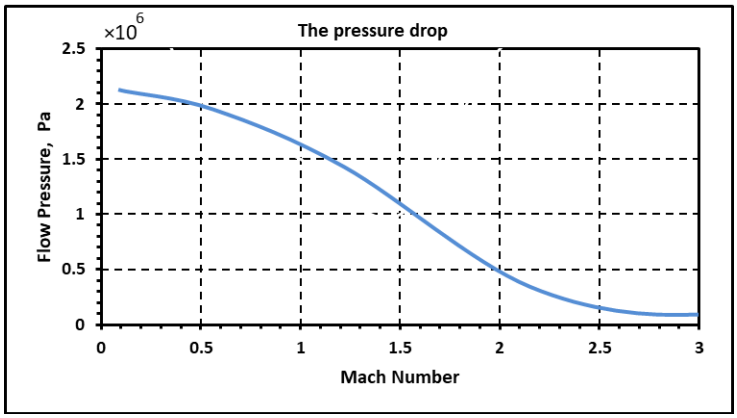

Fig. 6. Pressure drops through the nozzle.

As a typical case, Fig. 6 shows that as the fluid density is decreased from 0.14 kg/m^3 to 0.01 kg/m^3, the drop sizes produced from the leading edge of the face sheet increase from 135 to 210 μ. As the density is further decreased, the leading edge disappears, and drops are only produced from the side edges. Measurements of these latter drops have been made for all fluid densities up to 0.24 kg/m^3. These results are consistent with previously concluded experimental data [17].

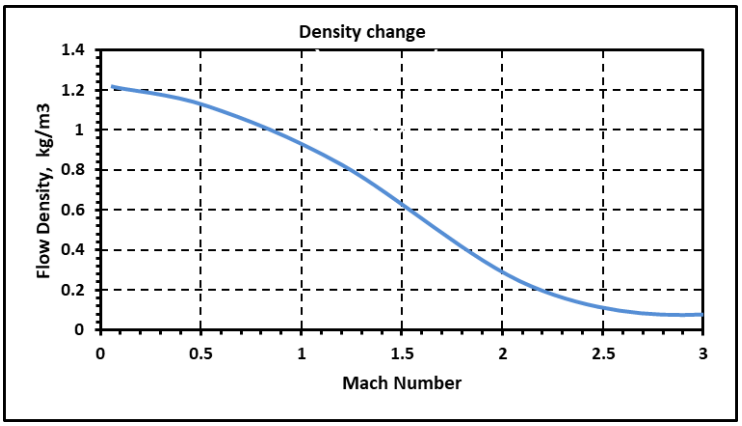

Fig. 7. Density changes through the nozzle.

Figure 8 shows the relationship of condenser back pressure at nozzle exit Ma of different entrainment ratios at condenser pressure. The net reduction condenser back pressure to fluid has been chosen as the comparison parameter at the basic value at a low fluid flow rate. In detail, the curves show a good agreement with increasing entrainment ratio. Also, the increase in fluid flow rate reduces condenser back pressure.

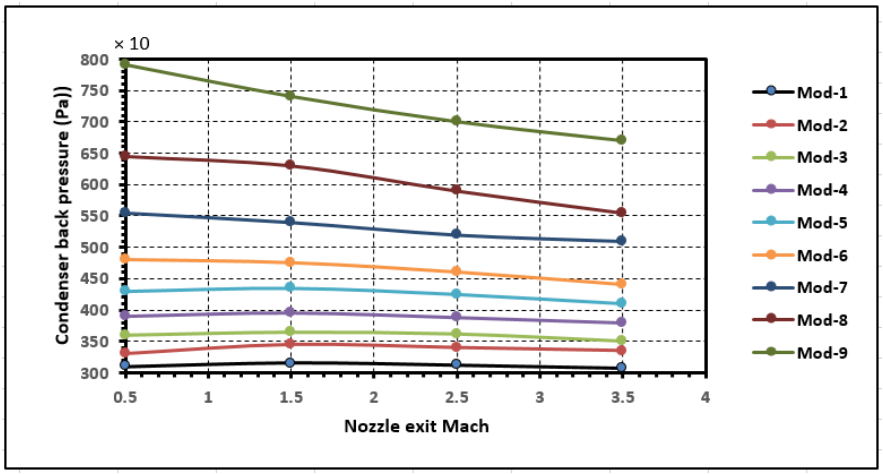

Fig. 8. Changing the nozzle exit Ma for different entrainment ratios with condenser pressure.

Figure 9 shows the coefficient of performance for the system model with condenser standard temperature in different cases. The coefficient of performance decreased with an increase in condenser temperature. It reached a 0.5 (50%) coefficient at a condenser temperature of 30 ºC, and 0.1 (10%) COP was the least performance recorded at fluid working at 43 ºC temperature. Figure 10 demonstrates the coefficient of performance for the system with condenser standard pressure in different cases.

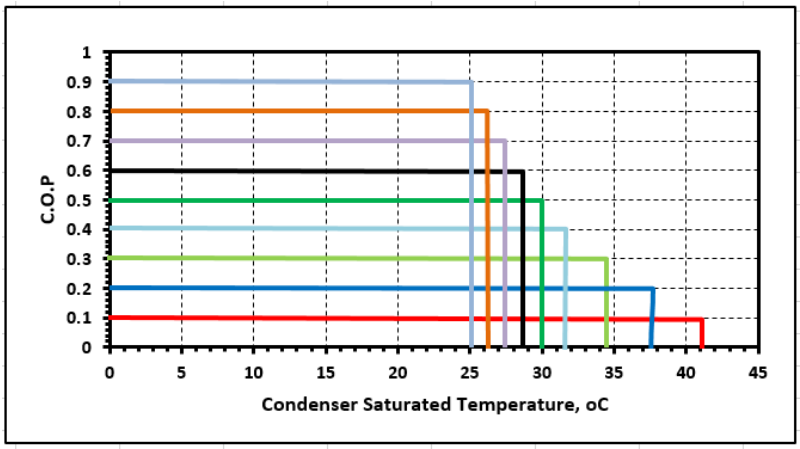

Fig. 9. The coefficient of performance with maximum condenser temperature operating limit.

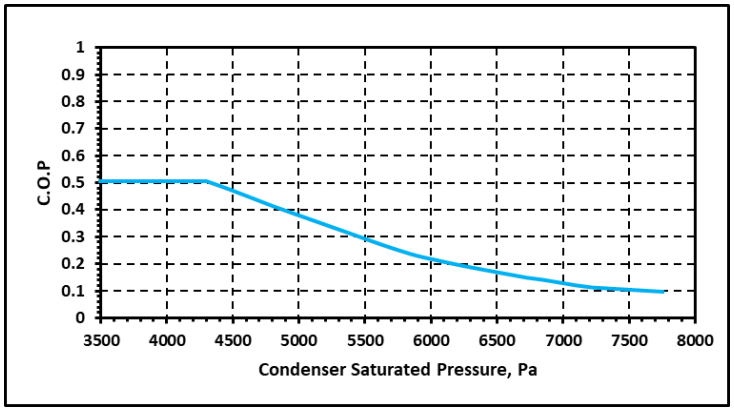

Fig. 10. Ejector (0.5) COP with condenser pressure.

4. Conclusions

Designing an ejector cooler system is complicated because it deals with many unknown parameters, such as the section area and mass flow rate. Creating a mathematical model to design the ejector is very important because it will be helpful to find good design parameters depending on the working range needs.

In addition, it is very important to reduce the time instead of directly building. Different models have been established to assess the ejector performance for different operating temperatures. However, during this study, the key to the design is that when the ejector operating temperature for the primary and secondary fluid of the boiler and the evaporator are below 100 ^{o}C, the coefficient of performance could be considered as same as the entrainment ratio according to the small difference in the latent heat.

Thus, fixing this ratio by using the constant pressure theory will enable us to deal with the rest of the design unknowns. The design results show that increasing the nozzle exit Mach number will increase the condenser saturated pressure to the critical pressure value. After that value, the pressure will reduce, causing the system's failure.

The problem is that increasing the COP of the ejector will limit the temperature working range for the condenser, and the opposite is true when the COP of the ejector decreases. The condenser's working temperature will be wide. It is important to know the design needs and works depending on that. However, when the condenser temperature is high, the effort and the cost of providing cooler fluid for the condenser will be reduced, which will be economically very good.

Nomenclatures

$A_{1,p}$	Nozzle exit area, m^2
$A_{1,s}$	Secondary flow section area at the nozzle exit, m^2
Am	Mixing chamber area, m^2
An	Nozzle area, m^2
At	Nozzle throat area, m^2
k	Hheat capacity ratio
m_m	Mixture mass flow rate , kg/s

m_p	Primary mass flow rate, kg/s
m_s	Secondary mass flow rate, kg/s
Ma	Nozzle Mach number
$Ma_{1,s}$	Secondary flow Mach number at the nozzle exit.
$Ma_{1.p}$	Primary flow Mach number at the nozzle exit.
Ma_3	Mixture Mach number.
Ma_4	Mach number after the shock wave.
$P_{1,p}$	Primary flow nozzle exit pressure, Pa
$P_{1.s}$	Secondary flow pressure at nozzle exit section, Pa
P_3	Mixture flow pressure, Pa
P_4	Pressure after shock wave, Pa
P_b	Condenser pressure- back pressure, Pa
$P_{o,p}$	Primary flow stagnation pressure, Pa
$P_{o,s}$	Secondary flow stagnation pressure, Pa
R	Ideal gas constant, kJ/kg.k)
$T_{o,p}$	Primary flow stagnation temperature, K
$T_{o,s}$	Secondary flow stagnation temperature, K
$T_{1,p}$	Primary flow temperature at the nozzle exit, K
T_3	Mixture flow temperature, K
v	Velocity, m/s
Greek Symbols	
ρ	Density, kg/m^3
$\dot{\eta}$	Efficiency
ω	Entrainment ratio

References

1. Sun, DW; and Eames I.W. (1995). Recent developments in the design theories and applications of ejectors-a review. *Journal of Institute Energy*, 68, 65-79.
2. Chunnanond, K.; and Aphornratana, S. (2004). Ejectors: applications in refrigeration technology. *Renewable Sustainable Energy Reviews*, 8(2), 129-155.
3. Zhang, X.J. and Wang, R.Z. (2022). A New Combined adsorption-ejector refrigeration and heating hybrid system powered by solar energy. *Applied Thermal Eng*ineering, 22, 1245-58.
4. He; S., Li; Y.; and Wang, R.Z. (2008). Progress of mathematical modelling on ejectors. *Renewable and Sustainable Energy Reviews*, 13(8), 1760-1780.
5. Huang; B.J.; Jiang, C.B.; Hu, F.L. (1985). Ejector performance characteristics and design analysis of jet refrigeration system. *ASME The American Society of Mechanical Engineers*, 0742-4795.
6. Scott, D.; Aidoun, Z.; and Ouzzane, M. (2011). An experimental investigation of an ejector for validating numerical simulations. *International Journal of Refrigeration*, 34, 1717-1723.
7. Mansour, R.B.; Ouzzane, M.; and Aidoun, Z. (2014). Numerical evaluation of ejector-assisted mechanical compression systems for refrigeration applications. *International Journal of Refrigeration*, 43, 46-49.

8. Lazarev; E.A.; Pomaz, A.N.; Salov, A.Y. (2016). System of ejection cooling of the charged air and evaluation of its effectiveness in the engine. *Procedia Engineering*, 150, 235-240.
9. Purjam, M.; Thu, K.; and Takahiko, M. (2021). Thermodynamic feasibility evaluation of a novel lowtemperature ejector-based trans-critical R744 refrigeration cycle. *EVERGREEN Joint Journal of Novel Carbon Resource Sciences & Green Asia Strategy*, 8(1), 204-212.
10. Pounds, D.A. (2010). A high efficiency ejector refrigeration system. Master Theses. University of Missouri, USA.
11. Malwe, P.D.; Gawali; B.S.; and Thakre, S.D. (2014). Exergy analysis of vapour compression refrigeration systems. *International Journal of Thermal Technologies*, 4(2), 54-57.
12. McGovern, J. A.; and Oladunjoye, S. (2015). Non-Intrusive second law performance evaluation of a domestic freezer. in *Proceedings of the 8th International Conference on Sustainable Energy and Environmental Protection—Part 2: State of the Art on Environmental Protection*, Olabi, A. G. and Alaswad, A. (Eds.), University of the West of Scotland, Paisley, UK, 48-53.
13. Yadav, P.; and Sharma, A. (2015). Exergy analysis of R134a based vapour compression refrigeration tutor. *IOSR Journal of Mechanical and Civil Engineering (IOSR-JMCE)* e-ISSN: 2278-1684, p-ISSN: 2320-334X, 73-77.
14. Prakash, U; Dr Vijayan, R; Vijay, P. (2016). Energy and exergy analysis of vapour compression refrigeration system with various mixtures of HFC/HC. *International Journal of Engineering Technology, Management and Applied Science* 4(1).
15. Mishra, S.; and Khan, M.E. (2016). Thermodynamic performance evaluation of single stage vapour compression system equipped with liquid vapour heat exchanger using eight ecofriendly refrigerants for reducing global warming. *International Journal of Science and Research*, 5(5), 49-55.
16. Tiwari, P.; Pandey, P.; and Rajput, S.P.S. (2017). Exergy analysis of domestic refrigerator by using alternate refrigerant. *International Research Journal of Engineering and Technology*, 4(5), 345-355.
17. Mahdi, L.A.; Mohammad, W.S.; and Mahmood, S.A. (2018). Exergy analysis of a domestic refrigerator. *Journal of Engineering*, 24(9).
18. Gill, J.; Singh, J.; Ohunakin, O.S.; and Adelekan, D.S. (2019). Exergy analysis of vapour compression refrigeration system using R450A as a replacement of R134a. *Journal of Thermal Analysis and Calorimetry*, 136(2), 857-872.
19. Kumar, N. (2019). Exergy analysis of VCR system with air-cooled condenser working with refrigerants R-134a and hydrocarbon. I*nternational Journal of Engineering and Advanced Technology*, 9(2), 2834-2839.
20. Abbady, K.; Al-Mutawa, N.; and Almutairi, A. (2023). New adapted one-dimensional mathematical and regression model to predict ejector performance. *International Journal of Heat and Technology*, 41(1), 151-161.
21. Bahajji, M.A.; Corberan, J.M.; Urchueguia, J.; Gonzalvez, J.; and Santiago, J. (2005). Study about the flashing process through a metering expansion valve. *Experimental Thermal and Fluid Science*, 29, 7577-63.
22. Ali, H.M.; Kadhim, S.A.; and Ibrahim, O.A. (2023). Evaluating refrigerant purity characteristics: an experimental approach to assess impact on vapor-

compression refrigeration system performance. *International Journal of Heat and Technology*, 41(4), 883-890.

23. Neverov, E.N.; Korotkiy, I.A.; Korotkih, P.S.; and Ivanova, L.A. (2023). Development of an energy efficient refrigeration unit using carbon dioxide as a natural refrigerant. *International Journal of Heat and Technology*, 41(5), 1151-1157.
24. Taslimitaleghani, S.; Sorin, M.; and Poncet, S. (2018). Energy and exergy efficiencies of different configurations of the ejector-based CO_2 refrigeration systems. *International Journal of Energy Production and Management*, 3(1), 22-33.
25. Boumaraf, L.; and Khadraoui, R. (2020). Investigation on the performance of a solar hybrid refrigeration system using environmentally friendly fluids. *International Journal of Heat and Technology*, 38(4), 960-966.